Published in final edited form as:
Biomacromolecules. 2013 April 8; 14(4): 976–985. doi:10.1021/bm301558q.

Switchable elastin-like polypeptides that respond to chemical inducers of dimerization

Jugal Dhandhukia[1], **Isaac Weitzhandler**[2,3], **Wan Wang**[1], and **J. Andrew MacKay**[1,4,*]

[1]Department of Pharmacology and Pharmaceutical Sciences

[2]Department of Chemical Engineering

[3]Department of Biomedical Engineering, Duke University, Pratt School of Engineering, Box 90271, Durham, NC 27708

[4]Department of Biomedical Engineering University of Southern California, School of Pharmacy, 1985 Zonal Avenue, Los Angeles, CA 90033-9121

Abstract

Elastin-like polypeptides (ELPs) are protein polymers that reversibly phase separate in response to increased temperature, pressure, concentration, ionic strength, and molecular weight. If it were possible to engineer their phase separation to respond to specific molecular substrates, ELP fusion proteins might be engineered as biosensors, smart biomaterials, diagnostic imaging agents, and targeted therapies. What has been lacking is a strategy to design ELPs to respond to specific substrates. To address this deficiency, we report that ELP fusion proteins phase separate in response to chemical inducers of dimerization (CID). The rationale is that ELP phase separation depends on molecular weight, concentration, and local hydrophobicity; therefore, processes that affect these properties, including non-covalent dimerization, can be tuned to produce isothermal phase separation. To test this hypothesis, constructs were evaluated consisting of an immunophilin: human FK-506 binding protein 12 (FKBP) attached to an ELP. Under stoichiometric binding of a CID, the fusion protein homodimerizes and triggers phase separation. This dimerization is reversible upon saturation with excess CID or competitive binding of a small lipophilic macrolide to FKBP. By modulating the ELP molecular weight, phase separation was tuned for isothermal response to CID at physiological ionic strength and temperature (37°C). To interpret the relationship between transition temperature and equilibrium binding constants, an empirical mathematical model was employed. To the best of our knowledge, this report is the first demonstration of reversible ELP switching in response to controlled dimerization. Due to its simplicity, this strategy may be useful to design ELP fusion proteins that respond to specific dimeric biological entities.

Keywords

Elastin-like Polypeptides; Human FK-506 Binding Protein 12; Chemical Inducers of Dimerization; Rapamycin

*Corresponding author: (jamackay@usc.edu) .

Supporting Information Available: A supplementary figure S1 has been prepared that shows the derivative of the optical density with respect to temperature, which was used to define the phase transition temperatures for ELP with and without the FKBP protein in presence of the CID ligand. This material is available free of charge via the Internet at http://pubs.acs.org.

Introduction

Protein switching is a critical triggering event in many biological signaling processes. However, using such events to trigger or modulate behavior of polymers remains challenging due to the complexity involved in the size, structure and nature of the polymer and ligand-protein pair. Herein, we report a fusion construct consisting of genetically engineered protein polymer linked to a fusion protein that homodimerizes upon binding of a bifunctional ligand known as a chemical inducer of dimerization (CID). CID's induce non covalent association between two hetero- or homologous proteins.[1, 2] The protein polymer belongs to a class of elastin-like polypeptides (ELPs) that respond to environmental properties including temperature, ionic strength, polymer concentration and pH.[3, 4] ELPs phase separate above an inverse phase transition temperature, T_t,[5, 6] which has properties similar to that displayed by polymers with lower critical solution temperatures. We demonstrate these fusion polypeptides reversibly phase separate when triggered by binding of a bifunctional ligand - B/B Homodimerizer (CID). This phase separation is specifically reversible upon competition with a lipophilic immunosuppressive macrolide - Rapamycin (Fig. 1).

Related studies have explored phase separation of protein-polymer fusions to control binding of ligand to the appended protein[7-11] as well as the reverse effect, that is, modulation of phase separation by allosteric ligand binding;[12] however, none of these approaches have identified dimerization as a mechanism to control phase separation. As such, it remains challenging to adopt previous findings to engineer fusion proteins that respond to new targets. In contrast, the formation of dimers is a simple approach to control ELP T_t, which has many potential applications due to the wide prevalence of multimeric target proteins, including antibodies, hemoglobin, tyrosine kinase receptors and cytokines, for instance, IL-5 and IL-10.[13, 14] Motivating this study, it remains to be seen if ELP fusion proteins that target dimeric species can be developed into smart polymers that switch from soluble (off) to insoluble (on) in response to their specific target.

To explore the potential applications of dimerization to design substrate-specific ELP-mediated phase separation, we engineered a fusion construct consisting of an immunophilin: FKBP attached to an ELP. ELPs are a class of protein polymers biologically inspired from human tropoelastin[15] which are composed of the repetitive pentameric amino acid sequence (Val-Pro-Gly-Xaa-Gly)$_l$ where Xaa and l control the ELP phase behavior. We selected ELPs as the environmentally responsive polymer for multiple reasons, including that they are amenable to genetic engineering using recursive directional ligation.[16] This enables biosynthesis of fusion constructs with precise control over chain length, protein position and the arrangement of fusion domains that might be challenging to prepare from synthetic polymers with LCST behavior, such as poly(N-isopropylacrylamide)[17] and poly(N-vinylcaprolactam).[18] Also, the ELP T_t can be modified by varying its guest residue[19] and chain length[3] which makes their sensitivity to the environment highly tunable.[20] Lastly, ELP tagged proteins can be purified from cellular expression systems using their thermal responsiveness.[21]

Given many options of homodimeric proteins to choose from, we selected FKBP because of its size and amphiphilic structural topology.[22] FKBP is a cytosolic receptor for immunosuppressive drugs, like FK-506 and Rapamycin, and plays a significant role in inhibiting T cell lymphokine gene activation.[23, 24] FKBP homodimerization has been well characterized and exploited in areas of transcription and signal transduction pathways.[25, 26] However, in this manuscript, we harness FKBP homodimerization to modulate polymer solubility in response to a CID switch. We hypothesized that at a fixed temperature, FKBP homodimerization by CID would trigger ELP phase separation due to an increase in local

ELP chain length and solvent-exposed hydrophobic area of FKBP-ELP dimer. FKBP is a soluble protein of ~ 12 kDa[27] in size and holds a hydrophobic ligand binding pocket[22] both of which may facilitate ELP-mediated phase separation. Previous studies on FKBP homodimerization in response to CID's such as AP1510 and FK1012A have been reported.[25, 28] Thus, FKBP can be used with a small library of CID's with various affinities, structures, and molecular weights. FKBP also has a strong affinity for Rapamycin (K_d = 0.2 nM),[24] which can specifically compete FKBP back to its monomeric state. CID applications have been reported in a range of cellular events inducing glycosylation, Wnt signaling, and apoptosis[29-31] but never, as per the best of our knowledge, have been used to trigger the phase separation of an ELP protein polymer.

Experimental Section

FKBP-ELP fusion gene design and synthesis

FKBP-ELP gene assembly was done in a two-step cloning process. pIDTsmart vector with the FKBP oligonucleotide sequence (the amino acid sequence of human FKBP previously been published)[32] was ordered from Integrated DNA technologies (IDT) with three restriction cut sites: NdeI, BserI and BamHI. The FKBP gene was flanked by restriction sites for NdeI and BserI with NdeI and BamHI cut sites at the 5′ and 3′ ends of the oligonucleotide respectively. The FKBP gene was cleaved from pIDTsmart vector using NdeI and BamHI cut sites and gel purified (GE Healthcare). The FKBP gene was then inserted into the pET25b (+) vector (Novagen) digested with same set of NdeI and BamHI enzymes. For the second step, FKBP gene was inserted into pET25b (+) vector containing the ELP gene using double digestion with BserI and BssHII cut sites.[33] The in-frame amino acid sequence of the fusion construct with FKBP attached to N terminus of ELP was confirmed by DNA sequencing.

FKBP-ELP protein expression and purification

E. coli BLR cells were transfected with pET25b (+) vector having the FKBP-ELP gene. Cells were inoculated onto ampicillin plates and incubated for period of 15-17 h at 37°C for optimum growth of bacterial colonies. A liter of bacterial culture was obtained by overnight inoculation with bacterial cells from 50 ml terrific broth starter media supplemented with 100 μg/mL ampicillin. The bacterial culture was centrifuged at 4000 rpm at room temperature, and the pellet obtained was re-suspended in cold PBS. The suspension was sonicated for cell lysis with a 10 sec on, 20 sec off pulse interval for a period of 3 min and the lysed product was centrifuged at 12,000 rpm at 4°C to discard any insoluble cellular debris. Polyethylene imine (0.5 %) was added to the supernatant for co-precipitation of DNA, incubated on ice for 15-20 min with occasional stirring and centrifuged again at 12,000 rpm at 4°C to remove any remnant insoluble cellular debris. The supernatant, which contains the fusion protein, was purified by Inverse Transition Cycling (ITC).[34] The fusion protein obtained was checked for its purity using SDS-PAGE (Fig. 2a).

FKBP-ELP characterization

The fusion construct obtained after ITC was calculated for its concentration using Beer Lambert's law at absorbance of 280 nm on a Nanodrop UV-Vis spectrophotometer with an estimated extinction coefficient of 11,585 $M^{-1}cm^{-1}$ using phosphate buffer saline (PBS) as the diluting solvent. Concentration range of 10-20 μg/μl was used for determining the molecular weight by running samples on 4-20% gradient Tris-Glycine-SDS PAGE gel under reducing conditions. Samples were stained with SDS loading buffer, denatured at 95°C for 5 mins and loaded onto SDS gel. Gels were stained using copper chloride solution (10% w/v) and imaged using a VersaDoc Gel Imager (Fig. 2a). The precise molecular weight of all constructs was confirmed by using MALDI-TOF (Table 1).

FKBP-ELP kinetics and transition temperature determination

The turbidity profiles of the samples were obtained using UV-Vis spectrophotometer. FKBP-ELP solutions with different B/B Homodimerizer (CID - Clontech, CA) concentrations were heated in Beckman Coulter Tm microcells (Brea, CA). The temperature was increased at rate of 1°C/min with readings taken every 0.3°C increments. Optical density at 350 nm was analyzed using the first derivative method and the maximum first derivative was defined as the phase transition temperature (Fig. 4 a, b, c, Supplementary Fig. S1). FKBP-ELP kinetic studies were performed on UV-Vis spectrophotometer by measuring OD at 350 nm as a function of time at a constant temperature by successive addition of stoichiometric amounts of CID and Rapamycin at predetermined fixed intervals (Fig. 5 a, b).

MALDI-TOF

The precise molecular weight of the fusion proteins was determined by MALDI-TOF (Table 1). Samples with 500μM concentration were prepared in a fresh saturated matrix solution of sinapic acid (50 mg in 7:3 ratio of acetonitrile to distilled water). An external control of albumin and apomyoglobin mixed with 1:1 ratio of matrix was prepared for calibration. All samples were loaded onto MALDI plate wells for drying at room temperature followed by determining its molecular weight by using weight - time of flight (TOF) principle on a mass spectrometer (Kratos Analytical).

Bio-layer Interferometry

The affinity of the CID towards FKBP-ELP was determined on a Blitz instrument (ForteBio, CA). To a 100 μM FKBP-ELP solution in PBS, 100 μM NHS-PEG_4-Biotin (Thermo Scientific) dissolved in distilled water was added. The mixture was incubated for 45 min at room temperature. Unreacted biotin was separated using Zeba Spin Desalting columns (7K MWCO, Thermo Scientific). The concentration of biotinylated FKBP-ELP was determined at absorbance of 280 nm using extinction coefficient of 11,585 $M^{-1}cm^{-1}$. Streptavidin biosensors were hydrated in PBS for at least 10 min before start of each run. A single run was divided into five distinct steps as follows: i) Baseline – where the streptavidin biosensor tip was immersed in PBS for 30 sec to obtain a zero baseline. ii) Loading – where 1 μM biotinylated FKBP-ELP was immobilized onto streptavidin-coated biosensor tip. This step was carried out for 180 sec, until the binding reached a plateau indicating maximum binding of biotinylated FKBP-ELP to streptavidin-coated biosensor tip. iii) Baseline – where the biosensor tip was again immersed in PBS for 30 sec to remove any unreacted biotinylated FKBP-ELP. iv) Association – where biotinylated FKBP-ELP biosensor tip was immersed in CID solution for a period of 240 sec. The data from this step was used to estimate differences in interference caused by binding of CID to biotinylated FKBP-ELP. v) Dissociation – where the FKBP-ELP-CID complex was immersed in PBS for 160 sec to dissociate the CID. Subsequent runs were performed with 0.05, 0.2, 1 and 2 μM CID solutions in PBS. Plain PBS was run as blank and subtracted from all sample readings. A new biosensor tip was used for every run. Data were analyzed using ForteBio Data Analysis package (Fig. 9).

Results and Discussion

Purification and phase behavior of FKBP-ELP fusion proteins

Two ELP constructs with Xaa = Val and l = 48 and 72 (V48, V72) and two FKBP fusion proteins (FKBP-V48, FKBP-V72) were purified from *E. coli* using Inverse Transition Cycling (ITC)[34] with yields of 80-100 mgs/L (Table 1). SDS-PAGE was used to determine the purity and molecular weights of all fusion constructs (Fig. 2a). The precise molecular weight of the fusion proteins was determined by MALDI-TOF (Table 1). Optical density

was used to characterize the temperature-concentration phase diagrams for each fusion protein (Fig. 2b). As observed in the figure, fusion to FKBP minimally influences the ELP transition temperatures, and the T_t follows an inverse relationship with logarithm of concentration.[3] Using the fit equation parameters for each of the fusion proteins (Fig. 2b, Table 1), it is possible to 'set' the T_t between 30 and 50 °C simply by selecting the appropriate fusion protein (FKBP-V48 or FKBP-V72) and adjusting the concentration (1-100 μM).

The ELP transition temperature responds to stoichiometric additions of CID

Given our hypothesis that a fusion between FKBP and an ELP protein polymer will exhibit switchable solubility upon ligand binding, we first tested the fusion protein sensitivity towards the CID. We chose the stoichiometric concentration CID: FKBP [1:2] as the starting point because theoretically each bifunctional CID should homodimerize two fusion proteins giving the maximal change in local concentration and hydrophobicity. A 5 μM FKBP-V48 solution in PBS was ramped from 15-60°C with and without (control) stoichiometric amount of CID. Binding of the CID to the fusion protein lowered the phase transition temperature by ~ 5-6°C as compared to the control group (Fig. 3 a, b). Similar results were obtained upon stoichiometric addition of CID to 4 μM FKBP-V72 which lowers the T_t by ~ 3-4°C as compared to the control group (Fig. 3 c, d). A plausible explanation for this observation is that FKBP dimerization acts as a bridge, roughly doubling the relative ELP chain length. In addition to increasing the ELP concentration associated with the complex, dimerization might also be accompanied by reduced number of interactions with the neighboring water molecules and a local increase in the hydrophobic environment of the FKBP/CID complex. Unliganded FKBP is associated with ordered water molecules in the hydrophobic binding cavity.[35] However, in presence of a related CID ligand, which dimerizes a mutant FKBP protein (F_M), enhanced hydrophobic contacts as well as hydrogen bonding and electrostatic interactions between the dimer have been observed.[36] In this study, CID likely induces a combination of FKBP-ELP dimerization and enhanced local hydrophobicity, which together result in substrate-dependent phase separation under isothermal conditions. As ELP phase separation depends on molecular weight and local polarity, both an increase in local ELP concentration and hydrophobicity may contribute to coacervation at reduced temperatures.[3, 37]

To further explore the responsiveness of ELP fusion proteins, we tested the behavior of FKBP-ELP at different CID concentrations. We observed that the fusion protein follows a biphasic competitive ligand-binding model. In particular, the fusion protein displays three trends: i) stoichiometric concentrations of CID results in the largest decrease in T_t; ii) above stoichiometry the system returns to the T_t values of the control group (without CID); and iii) below stoichiometry T_t increases incrementally towards the control group as observed for 5 μM FKBP-V48 (Fig. 4a). This illustration supports our initial hypothesis in three ways: First, at stoichiometric CID concentrations, one bifunctional CID homodimerizes two FKBP-ELP fusion proteins giving the maximal concentration of homodimers and the largest decrease in phase transition temperature. Second, at increasing concentrations, the CID's compete with each other to occupy FKBP binding sites and in doing so, each FKBP binding pocket becomes occupied by a CID. At saturating concentrations, no two free FKBP binding pockets are available to form the homodimer and thus the complex phase separates at temperatures similar to the control group. Third, with CID concentrations below stoichiometry, fewer homodimers are formed because of lack of sufficient CID molecules and the observed T_t increases. A similar trend is observed for 2.5 μM FKBP-V72 with CID concentrations above and below stoichiometry (Fig. 4b). A control of 5 μM V48 (without FKBP) in PBS with different CID concentrations was evaluated similarly. There was no change in T_t in samples with CID when compared to that of control (Fig. 4c). Taken

together, this suggests that the decrease in T_t observed with FKBP-ELP fusion protein (Fig. 3) occurs due to FKBP homodimerization in response to binding of its CID substrate. Thus, from these findings, we observe that FKBP-ELP is not only sensitive to the CID, but actually responds in a biphasic manner, whereby by adjusting the concentration of the ELP fusion protein it may be possible to detect either a decrease or an increase in the target CID concentration.

Reversible switching of FKBP-ELP at isothermal conditions

Having determined the specificity and stoichiometry of the FKBP-ELP phase separation in response to CID concentration, we next explored the isothermal reversibility of the switch using Rapamycin as a monomeric FKBP ligand. This was demonstrated by measuring optical density of the fusion proteins at 350 nm as function of time on a UV-Vis spectrophotometer with subsequent addition of stoichiometric amounts of CID and Rapamycin at predetermined fixed intervals. A 5 μM FKBP-V48 solution in PBS was stabilized at temperature of 46°C and temperature was held constant thereafter. Stoichiometric addition of 2.5 μM CID led to an increase in particulate turbidity as demonstrated by an increase in optical density to ~ 0.45, which returned to baseline levels on stoichiometric addition of 5 μM Rapamycin (Fig. 5a). The reversibility of the switch may be attributed to the stronger affinity of Rapamycin for monomeric FKBP compared to the CID. On addition of stoichiometric amounts of Rapamycin, it displaces the CID and in doing so, it disrupts the homodimer. This returns the system to the phase transition temperature observed for FKBP-ELP monomers, similar to that observed before addition of CID. The reverse ELP phase separation presumably occurs due to a decrease in the bridging of ELPs and return of the native FKBP state with increased polarity at the FKBP/CID interface as well as a decrease in the local concentration of ELP. Binding of Rapamycin to bovine FKBP has been shown to produce local changes in protein conformation and mobility.[35] Furthermore, the atomic structure of recombinant hFKBP with Rapamycin is associated with tightly bound water molecules.[38] This suggests a possible role for the increased polarity of FKBP-ELP-Rapamycin complex relative to CID-bound FKBP-ELP dimer. Under isothermal conditions, this competition from Rapamycin thus reverses ELP to their soluble form. Because solubility of Rapamycin in water is negligible (~ 3 μM),[39] a 36% v/v ethanol in water solution of Rapamycin was prepared for its solubilization and used to demonstrate the reversibility of the protein switch. A control was performed using 36% v/v of ethanol (without Rapamycin), adding an amount equivalent to that used in the sample group. The control was run to demonstrate that the reversibility of the switch was not due to a solubilizing effect of trace ethanol but rather due to specific disruption of the homodimer, successively reversing ELP phase separation. Isothermal switching was performed at 46°C because FKBP-V48 (5 μM) phase separates above and below 46°C in absence and presence of CID respectively (Fig. 3b).

To demonstrate that isothermal switching is not limited to FKBP-V48 and show that reversible phase separation can occur at physiological body temperature; we repeated these experiments with the fusion construct FKBP-V72 (4 μM) at 37°C (Fig. 3d). For this construct, optical density rose up to ~0.45 upon addition of 2 μM CID and returned to baseline upon successive addition of 4 μM Rapamycin (Fig. 5b). This data shows that it is possible to develop switchable ELP fusion polymers that are reversible under isothermal conditions at any target temperature, simply by modulating ELP chain length and concentration.

Quantitative modeling of FKBP-ELP switching behavior

Similar to a mathematical model that relates ELP phase behavior to its molecular architecture;[40] we developed a quantitative model that predicts the phase transition behavior

based on the FKBP-ELP fusion homodimerization. We began by quantifying the amount of FKBP-ELP in the dimeric or monomeric state at any given concentration of fusion protein and CID. The fusion protein's interaction with CID is assumed to occur via a two-step mechanism. First, one FKBP-ELP protein binds one CID. Then, the FKBP-ELP-CID complex binds a second FKBP-ELP protein to form a homodimer (Fig. 6). Eq. 1 and Eq. 2 represent the two reactions where free FKBP-ELP is denoted as 'P', free CID is denoted as 'L', FKBP-ELP-CID is denoted as 'PL', and the homodimer is denoted as 'P_2L'.

$$P+L<--->PL \quad \text{(Eq.1)}$$

$$PL+P<--->P_2L \quad \text{(Eq.2)}$$

Both steps are reversible, with distinct dissociation constants K_{d1} and K_{d2}. Assuming the system reaches equilibrium, Eq. 3 and Eq. 4 define K_{d1} and K_{d2}. Square brackets denote concentration.

$$K_{d1} = [P][L] / [PL] \quad \text{(Eq.3)}$$

$$K_{d2} = [PL][P] / [P_2L] \quad \text{(Eq.4)}$$

Given the total concentration of FKBP-ELP as C_{ELP} and CID as C_{CID}, applying a mass balance to each species yields Eq. 5 and Eq. 6.

$$C_{ELP} = [P] + [PL] + 2[P_2L] \quad \text{(Eq.5)}$$

$$C_{CID} = [L] + [PL] + [P_2L] \quad \text{(Eq.6)}$$

Eqs. 3, 4, 5, and 6 can be solved numerically for [P], [PL], [P_2L], and [L], thus allowing us to quantify the amount of FKBP-ELP that is 'switched on' [P_2L] or 'switched off' [P], [PL] at any total concentration of fusion protein and CID. To simplify the use of the above expressions, we define the fraction of ELP fusion protein that exists in the homodimeric state, f, as follows:

$$f = \frac{2[P_2L]}{C_{ELP}} \quad \text{(Eq.7)}$$

Subject to the magnitudes of K_{d1} and K_{d2}, f can be controlled by changing the total concentration of FKBP-ELP fusion protein, C_{ELP} and the total concentration of the chemical inducer of dimerization, C_{CID}.

In addition to possible contributions from the polarity of the local environment, ELP transition temperature depends on molecular weight and concentration; both of which change during formation of the homodimeric species. Meyer and coworkers developed an empirical model to describe the phase transition temperature as a function of chain length, sequence identity, and concentration.[3] We further developed Meyer's model to incorporate the concentration of FKBP-ELP that is 'on' and 'off' in order to quantify the relationship between [P], [L], [PL], and [P_2L], and the phase transition temperatures. Ultimately, this model allows the prediction of ELP phase behavior, which will be essential to deliberately design ELP fusions that phase separate in response to a specific concentration of a CID at a given temperature. Meyer's model relies on three constants—a critical transition temperature (T_c), a critical concentration (C_c), and a constant (k) with units of °C pentamers as follows:

$$T_t = T_c + \left(\frac{k}{l}\right) \ln\left(\frac{C_c}{C_{ELP}}\right) \quad \text{(Eq.8)}$$

The data in Figure 2b for ELPs with and without FKBP were fit to Eq. 8 (Table 2); furthermore, these are in agreement with numbers reported for ELPs with Xaa = Val.[3] To incorporate the relationship between FKBP-ELP and CID concentration into this model, Eq. 8 was combined with a series of assumptions as follows: i) the phase behavior of the monomer and dimeric species will both follow the solution for Eq. 8 (Table 2); ii) when $f = 1$, dimerization is accompanied by a 2 fold decrease in the concentration; iii) subject to Eqs. 3, 4, 5 and 6, f depends on the relative concentrations of the FKBP-ELP and the CID; and iv) the change in transition temperature between the monomeric and dimeric species can be approximated by a linear relationship as follows:

$$T_t = (1 - f)\, T_{t,\text{monomer}} + f T_{t,\text{dimer}} \quad \text{(Eq.9)}$$

This above approximation assumes that the whole system phase separates at a single phase transition temperature and that this is a linear interpolation between the transition temperature for 100% monomer and 100% dimer. This assumption was made for three reasons: i) for mixtures of FKBP-ELP and CID below stoichiometric ratios, only a single transition temperature was observed (Fig. 4 a, b, Supplementary Fig. S1); ii) the phase transition temperature for FKBP-ELPs followed a continuous-- not stepwise-- shift between the phase transition temperature of the dimer and the monomer; and iii) a posteriori, this assumption fit the data well. Since the whole system phase separates simultaneously, linear interpolation (Eq. 9) was selected to relate the phase transition temperature of the entire system to the monomer and dimer transition temperatures, which are given as follows:

$$T_{t,\text{monomer}} = T_c + \left(\frac{k}{l}\right) \ln\left(\frac{C_c}{C_{ELP}}\right) \quad \text{(Eq.10)}$$

and

$$T_{t,\text{dimer}} = T_c + \left(\frac{k}{2l}\right) \ln\left(\frac{C_c}{\frac{C_{ELP}}{2}}\right) \quad \text{(Eq.11)}$$

where l is length in pentamers of monomer and $2l$ is the length ELP associated with the homodimer. In the case where $f = 1$, then the ELP concentration would be C_{ELP} divided in half. Substitution of Eqs. 10 and 11 into Eq. 9, followed by simplification yields the following relationship:

$$T_t = T_c + \frac{k}{l}\left[\left(1 - \frac{f}{2}\right) \ln\left(\frac{C_c}{C_{ELP}}\right) + \left(\frac{f}{2}\right) \ln(2)\right] \quad \text{(Eq.12)}$$

Where in the case that f = 0, Eq. 12 reduces to Eq. 10, and if f = 1 then Eq. 12 reduces to Eq. 11. Values for the model parameters T_c, k and C_c were obtained using nonlinear regression to Eq. 8 to the set of FKBP-ELP transition temperatures, concentrations, and lengths (Fig. 2b, Table 2).

Modeling results

The model described above was fit to the experimental data set of 5 μM FKBP-V48 (shown in Fig. 4a). Least squares fitting by numerical iteration was used to estimate the values for K_{d1} and K_{d2} that gave an optimal fit (Fig. 7a). As demonstrated in the figure, the optimal fit

was obtained with K_{d1} equal to 230 nM and K_{d2} equal to 2.0 μM. Given those parameters, the model predicts the biphasic inverse phase transition temperature of FKBP-ELP fusion protein with a correlation coefficient of $R^2 = 0.76$. To confirm the validity of the model, it was also fit to the experimental data set of 2.5 μM FKBP-V72 (shown in Fig. 4b). Using least squares fitting by numerical iteration, the values for K_{d1} and K_{d2} were found to be 215 nM and 2.7 μM respectively which yield a fit with a correlation coefficient of $R^2 = 0.70$ (Fig. 7b).

To further elucidate the differences between K_{d1} and K_{d2}, we used our model to generate a plot of expected transition temperatures for FKBP-V72 as a function of CID concentration while varying the ratio between K_{d1} and K_{d2} (Fig. 7c). This plot indicates how for cases where $K_{d2}/K_{d1} = 1$, a more significant downward shift in the transition temperature would be expected than was observed (Fig. 7b). Intuitively, it makes sense that the two binding constants are different. The first binding event is the unhindered interaction of a small molecule (CID) with a large hydrophobic face of a single FKBP. In contrast, the second binding constant is the result of two FKBP domains coming into close proximity. Unlike naturally dimeric proteins, the FKBP proteins are not complementary. Instead, to dimerize via the CID, they must overcome additional steric hindrance. Thus, this data suggests that for the FKBP/CID system, K_{d1} is less than K_{d2}.

The predicted concentration of each form of FKBP-ELP, that is, [P], [PL], and [P_2L] is plotted against CID concentration for both the fusion proteins: 5 μM FKBP-V48 and 2.5 μM FKBP-V72 (Fig. 8 a, b). These figures estimate how much of the FKBP-ELP is in monomeric and dimeric form at any given CID concentration, and support our hypothesis of competitive ligand binding model (as observed in Fig. 4 a, b). As shown in the figure, we observe that at zero concentration of CID, all FKBP-ELP is in free monomeric form. As the CID is added, the concentration of free FKBP-ELP [P] drops quickly, as individual monomers bind to CID molecules. The concentration of FKBP-ELP-CID [PL] starts increasing until a particular CID concentration (stoichiometric amount) is reached, where the concentration of homodimeric FKBP-ELP [P_2L] is highest. Beyond stoichiometry, at saturating concentrations of CID, each FKBP-ELP molecule's binding site is occupied by its own CID molecule. As the concentration of FKBP-ELP-CID [PL] increases, the concentration of homodimer [P_2L] decreases, and we observe the reverse effect. These figures confirm that the highest concentration of homodimer [P_2L] does in fact occur when the concentration of CID is at stoichiometry. This model validates our understanding of the FKBP-ELP switching behavior. In particular, it indicates that the two-step reaction mechanism accurately describes the observed data and that the biphasic phase separation can be mediated by the stoichiometry of FKBP binding to a CID.

Model limitations

This model is designed to predict the transition temperature for a system of ELP monomers and homodimeric complexes. The optical density measurements used to generate Figures 2, 3, 4, and S1, revealed only a single major transition temperature for mixtures of ELP and CID. For this reason, a linear interpolation model (Eq. 9) was selected to model the transition temperature (Eq. 8). While the data suggest that all ELP fusion proteins phase separate at a single transition temperature, limitations in the interpretation of optical density prevent us from determining if monomeric species phase separate simultaneously with homodimeric ELP complexes. Thus, this model is limited by the assumption that the whole system phase separates at a single temperature. Similarly, the empirical model (Eq. 8) used to calculate transition temperatures only incorporated factors resulting from local molecular weight/concentration. Thus this model neglects possible contributions by local hydrophobicity at the FKBP/CID interface. The model also neglects possible contributions resulting from the phase separation of multi-block architectures, such as ELP-FKBP/CID/

FKBP-ELP. Next, we only demonstrated the accuracy of this model in predicting fusion protein behavior with ELPs containing valine as the guest residue. Lastly, this model relies on an assumption that the FKBP-ELP mixture reaches equilibrium in solution. Despite these limitations, the ability of this model to fit the observed data suggests that these assumptions are generally useful.

CID binding kinetics over immobilized FKBP-ELP

To further validate the above model, an independent measurement was used to estimate the equilibrium disassociation constant, K_{d1}, of the CID towards FKBP-ELP using Bio-layer Interferometry (BLI). BLI is a label-free analytical technique that measures binding kinetics in real time using microliter amounts of sample. BLI technology determines the change in interference pattern of white light reflected by binding of molecules onto the biosensor tip. This binding produces a shift in the interference pattern, which is recorded in nanometers (nm) by the instrument. NHS-PEG_4-Biotin was conjugated to exposed lysine groups of FKBP-ELP fusion protein using NHS-ester chemistry; furthermore, this material was immobilized on a streptavidin coated BLI biosensor tip. The experiment was designed to determine the binding kinetics of the first binding event where CID binds to FKBP-ELP giving FKBP-ELP-CID complex. Biotinylated FKBP-V72 was immobilized onto streptavidin biosensors followed by subsequently immersing the biosensor tips into CID solutions and PBS to measure the binding kinetics. Four different CID concentrations were used for the binding assay – 0.05, 0.2, 1 and 2 μM. The magnitude of the binding signal depended on the CID concentration (Fig. 9). A global fit was done to determine K_{d1}, k_{on} and k_{off} as 243 nM, 2.00×10^4 $M^{-1}s^{-1}$ and 4.85×10^{-3} s^{-1} respectively. Taking into consideration the design of the experiment, the affinity constant K_{d1} determined by BLI assay proved to be in relative agreement with that determined in the quantitative model (Fig. 7b). Due to the limitations of the instrument, BLI was unable to directly estimate the second and weaker dissociation constant, K_{d2}; however, the agreement between independently obtained values for K_{d1} from BLI and the quantitative model strengthens our hypothesis that FKBP-ELP interaction with CID is a two-step mechanism with two binding events.

Conclusion

This manuscript describes a rational strategy to design ELP protein polymers that changes solubility in response to small molecule ligands that induce ELP dimerization. To explore this approach, small molecules including both CID and Rapamycin were shown to bind to FKBP-ELP fusion proteins and induce sharp, reversible changes in the polypeptide solubility. A quantitative model was used to validate the biphasic relationship between the CID-dependent phase diagrams for two fusion proteins. This strategy to design switchable protein polymers has three distinct advantages over any yet proposed. First, it provides a logical approach to detect classes of target molecules that mediate dimerization via substrate-specific interaction with an ELP protein fusion. While we have evaluated this approach to detect small molecule CID's, this strategy might similarly detect multimeric protein targets. Second, because the response to CID concentration is biphasic, by adjusting the ratio between the ELP and CID this strategy can induce either association or dissociation in response to a respective increase or decrease in CID concentration. Third, the isothermal response to CID can be modulated to occur at any temperature between 30 and 50°C by adjusting the ELP molecular weight or concentration. ELPs of other amino acid sequences may permit a wider range for isothermal switching; therefore, switching may be adaptable to refrigeration, ambient, or physiological temperatures. Having demonstrated the feasibility of this strategy, it may now be possible to engineer environmentally responsive protein polymers that phase separate in response to multimeric target substrates. Due to the

adaptability and specificity of this strategy, these fusion protein polymers may be evaluated for diverse applications in the detection and treatment of diseases.

Supplementary Material

Refer to Web version on PubMed Central for supplementary material.

Acknowledgments

This work was made possible by the University of Southern California, the National Institute of Health R21EB012281, P30 CA014089 to the Norris Comprehensive Cancer Center, the Wright Foundation, the Stop Cancer Foundation, the American Cancer Society, the USC Ming Hsieh Institute to J.A.M., the USC Nanobiophysics Core Facility, and the Translational Research Laboratory at the School of Pharmacy.

References

1. Austin DJ, Crabtree GR, Schreiber SL. Proximity verses allostrey: the role of regulated protein dimerization in biology. Chem Biol. 1994; 1:131. [PubMed: 9383382]
2. Pastuszka MK, Mackay JA. Biomolecular engineering of intracellular switches in eukaryotes. J Drug Deliv Sci Technol. 2010; 20(3):163–169. [PubMed: 21209849]
3. Meyer DE, Chilkoti A. Quantification of the effects of chain length and concentration on the thermal behavior of elastin-like polypeptides. Biomacromolecules. 2004; 5(3):846–851. [PubMed: 15132671]
4. Mackay JA, Callahan DJ, Fitzgerald KN, Chilkoti A. Quantitative Model of the Phase Behavior of Recombinant pH-Responsive Elastin-Like Polypeptides. Biomacromolecules. 2010
5. Urry DW. Entropic elastic processes in protein mechanisms. I. Elastic structure due to an inverse temperature transition and elasticity due to internal chain dynamics. J Protein Chem. 1988; 7(1):1–34. [PubMed: 3076447]
6. Urry DW. Free energy transduction in polypeptides and proteins based on inverse temperature transitions. Prog Biophys Mol Biol. 1992; 57(1):23–57. [PubMed: 1549698]
7. Stayton PS, Shimoboji T, Long C, Chilkoti A, Chen G, Harris JM, Hoffman AS. Control of protein-ligand recognition using a stimuli-responsive polymer. Nature. 1995; 378(6556):472–4. [PubMed: 7477401]
8. Ding Z, Fong RB, Long CJ, Stayton PS, Hoffman AS. Size-dependent control of the binding of biotinylated proteins to streptavidin using a polymer shield. Nature. 2001; 411(6833):59–62. [PubMed: 11333975]
9. Shimoboji T, Ding ZL, Stayton PS, Hoffman AS. Photoswitching of ligand association with a photoresponsive polymer-protein conjugate. Bioconjug Chem. 2002; 13(5):915–9. [PubMed: 12236771]
10. Shimoboji T, Larenas E, Fowler T, Hoffman AS, Stayton PS. Temperature-induced switching of enzyme activity with smart polymer-enzyme conjugates. Bioconjug Chem. 2003; 14(3):517–25. [PubMed: 12757374]
11. Shimoboji T, Larenas E, Fowler T, Kulkarni S, Hoffman AS, Stayton PS. Photoresponsive polymer-enzyme switches. Proc Natl Acad Sci U S A. 2002; 99(26):16592–6. [PubMed: 12486222]
12. Kim B, Chilkoti A. Allosteric actuation of inverse phase transition of a stimulus-responsive fusion polypeptide by ligand binding. J Am Chem Soc. 2008; 130(52):17867–73. [PubMed: 19055326]
13. Kusano S, Kukimoto-Niino M, Hino N, Ohsawa N, Ikutani M, Takaki S, Sakamoto K, Hara-Yokoyama M, Shirouzu M, Takatsu K, Yokoyama S. Structural basis of interleukin-5 dimer recognition by its alpha receptor. Protein Sci. 2012; 21(6):850–64. [PubMed: 22528658]
14. Zdanov A, Schalk-Hihi C, Gustchina A, Tsang M, Weatherbee J, Wlodawer A. Crystal structure of interleukin-10 reveals the functional dimer with an unexpected topological similarity to interferon gamma. Structure. 1995; 3(6):591–601. [PubMed: 8590020]

15. Urry DW, Okamoto K, Harris RD, Hendrix CF, Long MM. Synthetic, cross-linked polypentapeptide of tropoelastin: an anisotropic, fibrillar elastomer. Biochemistry. 1976; 15(18): 4083–9. [PubMed: 963023]
16. McDaniel JR, Mackay JA, Quiroz FG, Chilkoti A. Recursive directional ligation by plasmid reconstruction allows rapid and seamless cloning of oligomeric genes. Biomacromolecules. 2010; 11(4):944–52. [PubMed: 20184309]
17. Chen JP, Yang HJ, Hoffman AS. Polymer-protein conjugates. I. Effect of protein conjugation on the cloud point of poly (N-isopropylacrylamide). Biomaterials. 1990; 11(9):625–30. [PubMed: 2090295]
18. Srivastava A, Kumar A. Thermoresponsive poly(N-vinylcaprolactam) cryogels: synthesis and its biophysical evaluation for tissue engineering applications. Journal of materials science. Materials in medicine. 2010; 21(11):2937–45. [PubMed: 20625836]
19. Urry DW, Gowda DC, Parker TM, Luan CH, Reid MC, Harris CM, Pattanaik A, Harris RD. Hydrophobicity scale for proteins based on inverse temperature transitions. Biopolymers. 1992; 32(9):1243–50. [PubMed: 1420991]
20. Pastuszka MK, Janib SM, Weitzhandler I, Okamoto CT, Hamm-Alvarez S, Mackay JA. A tunable and reversible platform for the intracellular formation of genetically engineered protein microdomains. Biomacromolecules. 2012; 13(11):3439–44. [PubMed: 23088632]
21. Meyer DE, Chilkoti A. Purification of recombinant proteins by fusion with thermally-responsive polypeptides. Nat Biotechnol. 1999; 17(11):1112–5. [PubMed: 10545920]
22. Main ER, Fulton KF, Jackson SE. Folding pathway of FKBP12 and characterisation of the transition state. Journal of molecular biology. 1999; 291(2):429–44. [PubMed: 10438630]
23. Sharma VK, Li B, Khanna A, Sehajpal PK, Suthanthiran M. Which way for drug-mediated immunosuppression? Curr Opin Immunol. 1994; 6(5):784–90. [PubMed: 7826535]
24. Bierer BE, Mattila PS, Standaert RF, Herzenberg LA, Burakoff SJ, Crabtree G, Schreiber SL. Two distinct signal transmission pathways in T lymphocytes are inhibited by complexes formed between an immunophilin and either FK506 or rapamycin. Proc Natl Acad Sci U S A. 1990; 87(23):9231–5. [PubMed: 2123553]
25. Amara JF, Clackson T, Rivera VM, Guo T, Keenan T, Natesan S, Pollock R, Yang W, Courage NL, Holt DA, Gilman M. A versatile synthetic dimerizer for the regulation of protein-protein interactions. Proc Natl Acad Sci U S A. 1997; 94(20):10618–23. [PubMed: 9380684]
26. Spencer DM, Wandless TJ, Schreiber SL, Crabtree GR. Controlling signal transduction with synthetic ligands. Science. 1993; 262(5136):1019–24. [PubMed: 7694365]
27. Aghdasi B, Ye K, Resnick A, Huang A, Ha HC, Guo X, Dawson TM, Dawson VL, Snyder SH. FKBP12, the 12-kDa FK506-binding protein, is a physiologic regulator of the cell cycle. Proc Natl Acad Sci U S A. 2001; 98(5):2425–30. [PubMed: 11226255]
28. Schultz LW, Clardy J. Chemical inducers of dimerization: the atomic structure of FKBP12-FK1012A-FKBP12. Bioorg Med Chem Lett. 1998; 8(1):1–6. [PubMed: 9871618]
29. Czlapinski JL, Schelle MW, Miller LW, Laughlin ST, Kohler JJ, Cornish VW, Bertozzi CR. Conditional glycosylation in eukaryotic cells using a biocompatible chemical inducer of dimerization. J Am Chem Soc. 2008; 130(40):13186–7. [PubMed: 18788807]
30. Shahi P, Park D, Pond AC, Seethammagari M, Chiou SH, Cho K, Carstens JL, Decker WK, McCrea PD, Ittmann MM, Rosen JM, Spencer DM. Activation of Wnt signaling by chemically induced dimerization of LRP5 disrupts cellular homeostasis. PLoS One. 2012; 7(1):e30814. [PubMed: 22303459]
31. Souza DS, Spencer DM, Salles TS, Salomao MA, Payen E, Beuzard Y, Carvalho HF, Costa FF, Saad ST. Death switch for gene therapy: application to erythropoietin transgene expression. Braz J Med Biol Res. 2010; 43(7):634–44. [PubMed: 20499015]
32. Standaert RF, Galat A, Verdine GL, Schreiber SL. Molecular cloning and overexpression of the human FK506-binding protein FKBP. Nature. 1990; 346(6285):671–4. [PubMed: 1696686]
33. Sun G, Hsueh PY, Janib SM, Hamm-Alvarez S, MacKay JA. Design and cellular internalization of genetically engineered polypeptide nanoparticles displaying adenovirus knob domain. Journal of controlled release : official journal of the Controlled Release Society. 2011; 155(2):218–26. [PubMed: 21699930]

34. Hassouneh W, Christensen T, Chilkoti A. Elastin-like polypeptides as a purification tag for recombinant proteins. Curr Protoc Protein Sci. 2010:11. Chapter 6, Unit 6. [PubMed: 20814933]

35. Wilson KP, Yamashita MM, Sintchak MD, Rotstein SH, Murcko MA, Boger J, Thomson JA, Fitzgibbon MJ, Black JR, Navia MA. Comparative X-ray structures of the major binding protein for the immunosuppressant FK506 (tacrolimus) in unliganded form and in complex with FK506 and rapamycin. Acta Crystallogr D Biol Crystallogr. 1995; 51(Pt 4):511–21. [PubMed: 15299838]

36. Rollins CT, Rivera VM, Woolfson DN, Keenan T, Hatada M, Adams SE, Andrade LJ, Yaeger D, van Schravendijk MR, Holt DA, Gilman M, Clackson T. A ligand-reversible dimerization system for controlling protein-protein interactions. Proc Natl Acad Sci U S A. 2000; 97(13):7096–101. [PubMed: 10852943]

37. Trabbic-Carlson K, Meyer DE, Liu L, Piervincenzi R, Nath N, LaBean T, Chilkoti A. Effect of protein fusion on the transition temperature of an environmentally responsive elastin-like polypeptide: a role for surface hydrophobicity? Protein engineering, design & selection : PEDS. 2004; 17(1):57–66.

38. Van Duyne GD, Standaert RF, Karplus PA, Schreiber SL, Clardy J. Atomic structures of the human immunophilin FKBP-12 complexes with FK506 and rapamycin. J Mol Biol. 1993; 229(1): 105–24. [PubMed: 7678431]

39. Simamora P, Alvarez JM, Yalkowsky SH. Solubilization of rapamycin. Int J Pharm. 2001; 213(1-2):25–9. [PubMed: 11165091]

40. Ghoorchian A, Holland NB. Molecular architecture influences the thermally induced aggregation behavior of elastin-like polypeptides. Biomacromolecules. 2011; 12(11):4022–9. [PubMed: 21972921]

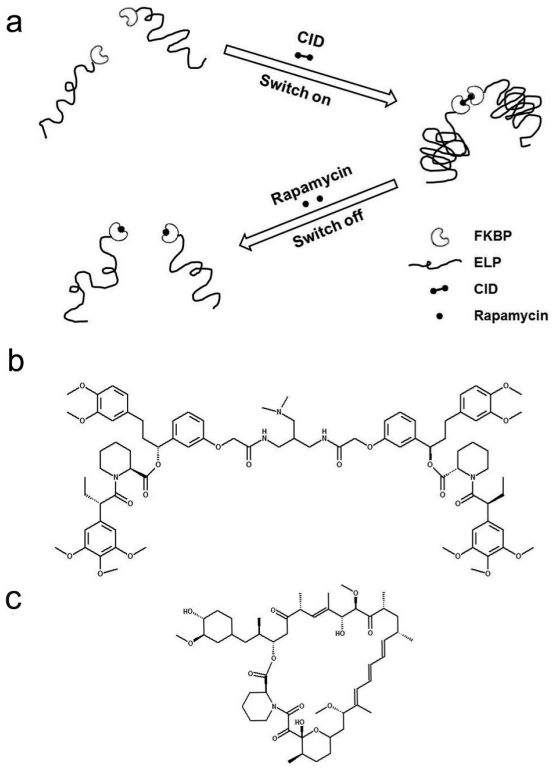

Figure 1. Reversible switching of FKBP-ELP fusion proteins by controlled dimerization

(a) Addition of a CID induces assembly of the fusion proteins, which can be reversed by competition with a high affinity substrate, Rapamycin. The dimeric fusion protein has a lower T_t; therefore, under isothermal conditions they phase separate in response to CID substrates. **(b)** Chemical structure of CID. **(c)** Chemical structure of Rapamycin.

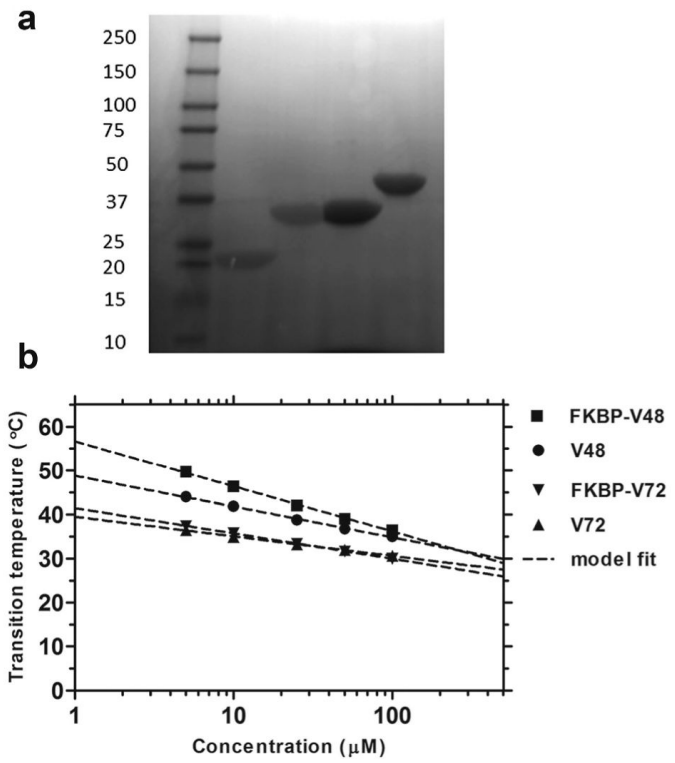

Figure 2. Characterization of ELP fusion proteins

(a) Copper-stained SDS-PAGE confirmed the identity and purity of fusion proteins. Samples appeared as single bands with V48 and V72 in lanes 2 and 3; and FKBP-V48 and FKBP-V72 in lanes 4 and 5 respectively. **(b)** Temperature-concentration phase diagrams measured optical density at 350 nm by warming the sample solution at the rate of 1°C/min. ELPs phase separate above the indicated lines.

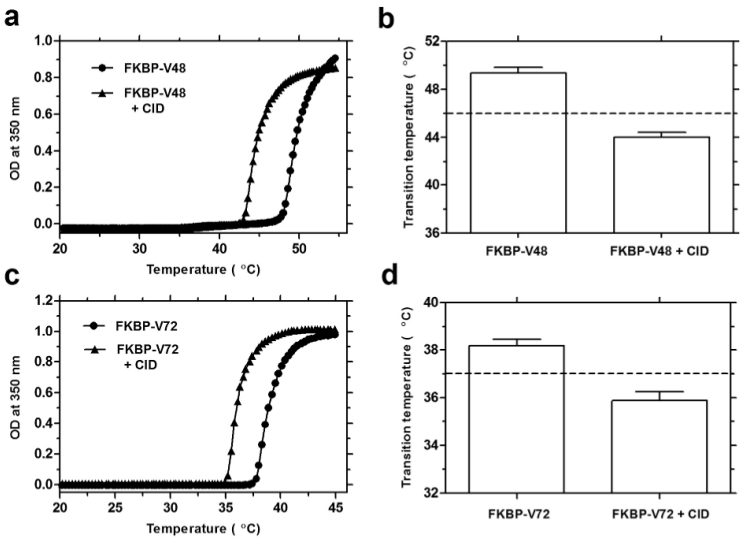

Figure 3. CID homodimerization to FKBP-ELP lowers its phase transition temperature

(a) Optical density profile of 5 μM FKBP-V48 in presence of stoichiometric amount of CID (filled triangles) and control (filled circles). **(b)** Decrease in transition temperature of 5 μM FKBP-V48 by stoichiometric CID binding (n = 3), Paired t-test, $p = 0.007$, $R^2 = 0.98$ **(c)** Optical density profile of 4 μM FKBP-V72 in presence of stoichiometric amount of CID (filled triangles) and control (filled circles). **(d)** Decrease in transition temperature of 4 μM FKBP-V72 by stoichiometric CID binding (n = 3), Paired t-test, $p = 0.023$, $R^2 = 0.95$.

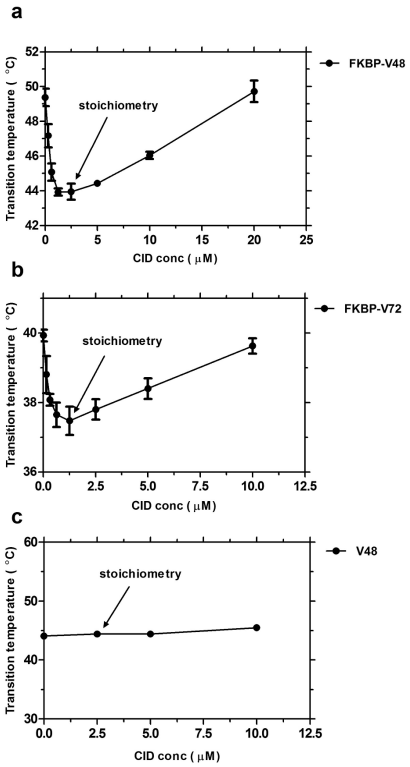

Figure 4. FKBP-ELP phase transition temperature depends on CID stoichiometry

(a) T_t values for 5 μM FKBP-V48 (n = 4) and **(b)** 2.5 μM FKBP-V72 (n = 4) decreases with increase in CID concentration until CID: FKBP reaches stoichiometry (permitting the maximal concentration of homodimers). Subsequent increase in the CID concentration competes apart homodimers and return the phase transition temperature back upwards. **(c)** 5 μM V48 with different CID concentrations showing no difference in T_t.

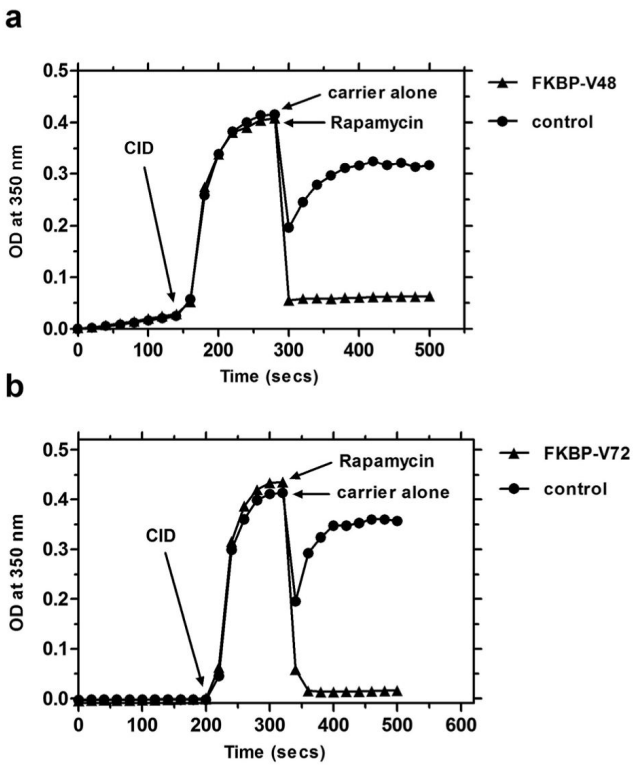

Figure 5. FKBP-ELP phase separation is fast and reversible under isothermal conditions

Phase separation was determined by measuring optical density as function of time using UV Vis kinetics. **(a)** Optical density profile of 5 μM FKBP-V48 (filled triangles) and control (filled circles) at 46 °C. **(b)** Optical density profile of 4 μM FKBP-V72 (filled triangles) and control (filled circles) at 37 °C. The results were seen after sequential addition of stoichiometric amounts of CID and Rapamycin as shown by arrows.

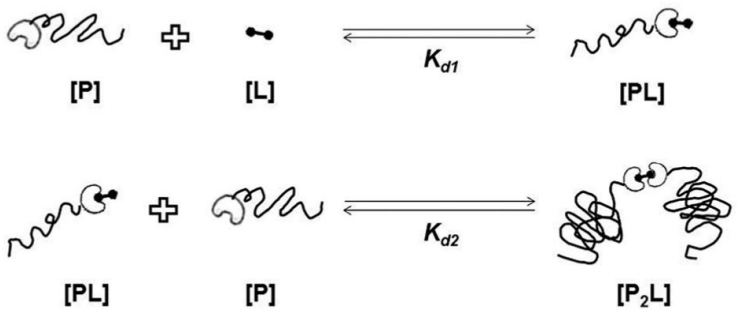

Figure 6. FKBP-ELP dimerization occurs via a two-step process

FKBP-ELP protein binds to one CID to give FKBP-ELP-CID complex which then binds to a second FKBP-ELP protein to give the homodimer.

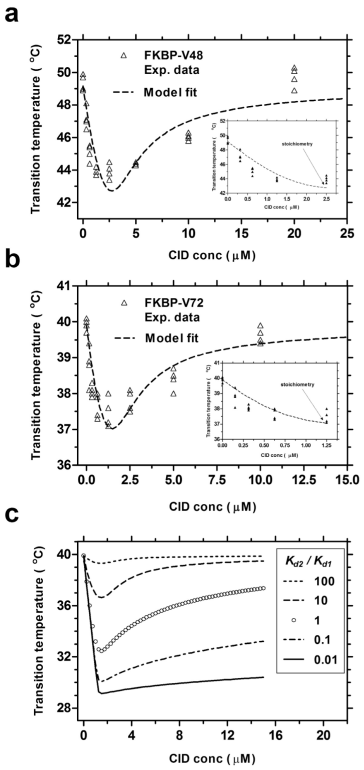

Figure 7. Quantitative model of FKBP-ELP switching behavior

(a) FKBP-V48 (5 μM) model fit with parameters K_{d1} = 230 nM, K_{d2} = 2.0 μM and R^2 = 0.76 and **(b)** FKBP-V72 (2.5 μM) model fit with parameters K_{d1} = 215 nM, K_{d2} = 2.7 μM and R^2 = 0.7. **(c)** To visualize the relationship between the shape of the curve and K_{d2}, the predicted transition temperature is indicated for FKBP-V72 (2.5 μM, K_{d1} = 215 nM) and varying the ratio of K_{d2}/K_{d1}.

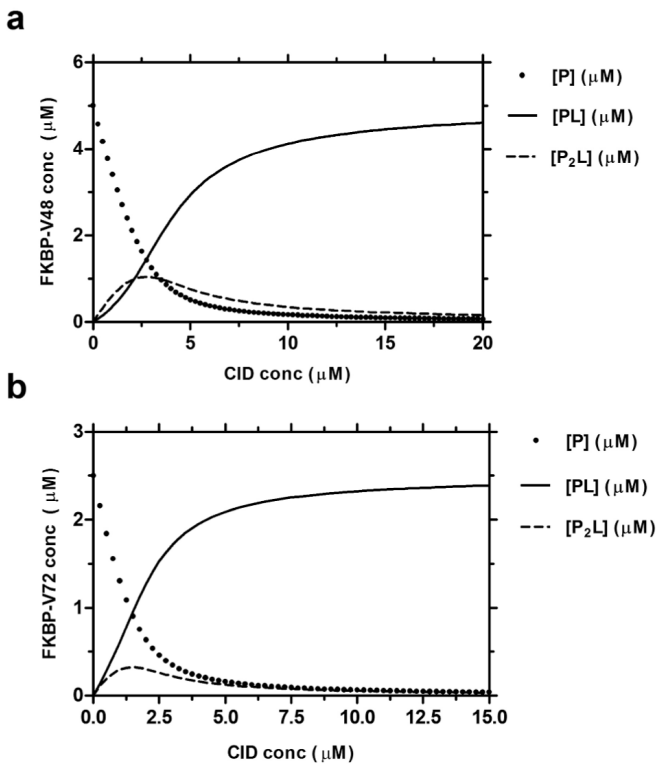

Figure 8. Predicted concentrations of FKBP-ELP species vs. CID concentration

Maximal concentration of homodimer formation [P_2L] occurs at stoichiometric concentrations of CID for **(a)** 5 μM FKBP-V48 and **(b)** 2.5 μM FKBP-V72.

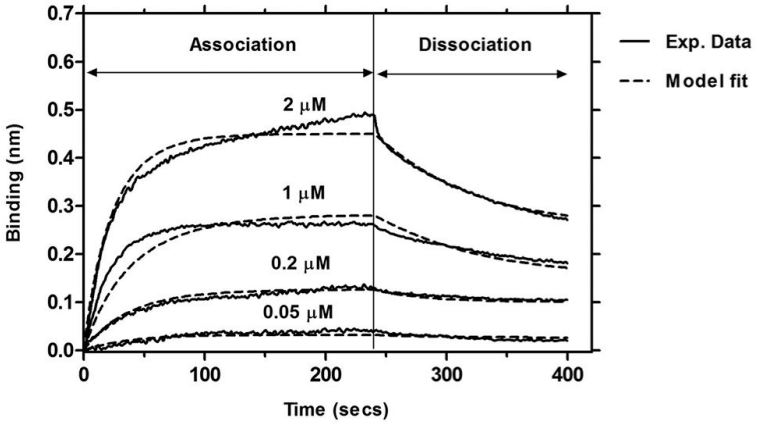

Figure 9. Binding of CID to FKBP-V72 shows strong association and fast dissociation kinetics

Association and Dissociation kinetics of CID solutions over immobilized FKBP-V72 yield a global fit with K_{d1} = 243 nM, k_{on} = 2.00×10^4 $M^{-1}s^{-1}$ and k_{off} = 4.85×10^{-3} s^{-1}.

Table 1

Physical properties of ELP protein polymers with and without FKBP

Label	[a]Amino acid sequence	Expected MW (kDa)	[b]Observed MW (kDa)	T_t at 25 μM (°C)	[c]Slope, m [°C Log (μM)]	[c]Intercept, b (°C)
V48	$MG(VPGVG)_{48}Y$	19.7	19.7	38.8	7.01	48.8
V72	$MG(VPGVG)_{72}Y$	29.5	29.6	33.2	4.45	39.5
FKBP-V48	$FKBP\text{-}G(VPGVG)_{48}Y$	31.5	31.4	42.0	10.26	56.7
FKBP-V72	$FKBP\text{-}G(VPGVG)_{72}Y$	41.3	41.3	33.4	5.76	41.5

[a]FKBP amino acid sequence:
MGVQVETISPGDGRTFPKRGQTCVVHYTGMLEDGKKFDSSRDRNKPFKFMLGKQEVIRGWEEGVAQMSVGQRAKLTISPD
YAYGATGHPGIIPPHATLVFDVELLKLE

[b]Dialyzed samples in water (500 μM) were mixed with acetonitrile saturated with sinapic acid, air dried, and characterized using MALDI-TOF.

[c]Phase diagrams were fit with the following linear relationship: $T_t = b - m[\text{Log}_{10}(\text{concentration})]$. Mean ± 95% CI. $R^2 = 0.99$.

Table 2

Fit parameters for temperature vs. interaction of length and concentration for ELP with and without FKBP fusion protein

	*FKBP-ELP (Xaa=Val)	*ELP (Xaa=Val)	**ELP (Xaa=Val)
T_c (°C)	15.5	21.7	20.8
k (°C pentamers)	203.5	144	129
C_c (μM)	14,120	8,008	25,000

*Data (Fig. 2b) fit to Eq. 8

**Reported values fit to Eq. 8